Proceedings of the ASME 2017 International Design Engineering Technical Conferences & Computers and Information in Engineering Conference
IDETC2017
August 6-9, 2017, Cleveland, Ohio, USA

DETC2017-67988

A FRICTION MODEL FOR NON-SINGULAR COMPLEMENTARITY FORMULATIONS FOR MULTIBODY SYSTEMS WITH CONTACTS

Albert Peiret
Dept. of Mechanical Engineering
and Centre for Intelligent Machines
McGill University, Montréal, Canada
Email: alpeiret@cim.mcgill.ca

József Kövecses
Dept. of Mechanical Engineering
and Centre for Intelligent Machines
McGill University, Montréal, Canada
Email: jozsef.kovecses@mcgill.ca

Josep M. Font-Llagunes
Dept. of Mechanical Engineering and
Biomedical Engineering Research Centre
UPC, Barcelona, Spain
Email: josep.m.font@upc.edu

ABSTRACT

The dynamics of multibody systems with many contacts are frequently formulated as a Linear Complementarity Problem (LCP), for which several direct or iterative algorithms are available to solve it efficiently. These formulations rely on discretized friction models that approximate the friction cone of the Coulomb model to a pyramid. However, they produce rank-deficient LCPs even though the physical problem does not have constraint redundancy and has a unique solution. Here, a new discretized friction model is presented which results in an LCP formulation with a full-rank lead matrix. This model relies on an inertial term to couple the equations of the model, which behaves as close to the Coulomb model as the other discretized models. Moreover, it is shown through some simulations that some algorithms can be used with this formulation, which could not be used with the other rank-deficient LCP formulations.

INTRODUCTION

The dynamics of multibody systems with contacts presents some well-known challenges, especially when it involves frictional contacts. If friction is neglected, the representation takes the form of a *linear complementarity problem* (LCP) [1], for which the existence of solution is guaranteed [2], and several direct or iterative solution algorithms are available in the literature. However, considering friction in contacts using the Coulomb model turns the formulation into a *nonlinear complementarity problem* (NCP), for which nonlinear optimization techniques need to be used [3], and the existence of solution is not always guaranteed.

Several friction models have been proposed to approximate the Coulomb model so that the model can take the form of an LCP [4–7]. These models are based on the discretized (or faceted) friction cone, which turns the nonlinear inequalities of the original model into linear ones by choosing a finite number of directions in the tangent plane. As a result, this discretized model approximates the friction cone with a pyramid (or faceted cone). It is worth mentioning that this issue is only related to the contact points that are not sliding, because the static friction force is confined to the friction cone; whereas the kinetic friction force is defined by a constitutive relation and it is possible to formulate an LCP [4].

Generally, the Coulomb model can be discretized using two different approaches: *discrete force* or *discrete acceleration*. The former parametrizes the friction force with non-positive components associated with the set of directions defined on the tangent plane, which are used to define the complementarity conditions with the tangent acceleration vector [5, 6]; while the latter parametrizes the acceleration with non-positive components to define the complementarity conditions with the static friction saturation along each direction [4]. The size of the problem to solve is very similar in both cases, and they can behave the same for certain sets of chosen directions. A common characteristic of these models in multibody system formulations is that the lead matrix of the LCP is rank deficient, even though there is no redundancy in the contact forces of the system. This is due to the

use of more than two non-independent directions in the tangent plane, and so it is an artifact of the model.

Several algorithms to solve LCP problems are available in the literature. *Direct* or *pivoting methods* are based on the *simplex methods*, such as Lemke, Murty, and Júdice and Pires [8–10]. However, most of these methods require a non-singular lead matrix to solve the LCP. Here, a new discretized friction model is proposed to approximates the Coulomb model, so that the formulated LCP has a full-rank lead matrix.

Unfortunately, the existence of a solution for the dynamic equations with Coulomb friction (i.e., forces and acceleration) is not guaranteed under some circumstances [11]. That is why the time-stepping is usually embedded in the equations, so that a solution always exists for impulses and velocities [5–7]. The LCP presented here with the new friction model has been formulated at the velocity level, and also compared with other formulations for multibody systems with contacts.

CONTACT MODEL

For each pair of surfaces in contact, the contact force components are arranged as follows

$$\boldsymbol{\lambda}_\mathrm{c} = \begin{bmatrix} \lambda_\mathrm{n} \\ \boldsymbol{\lambda}_\mathrm{t} \end{bmatrix} \tag{1}$$

where λ_n is the normal contact force and $\boldsymbol{\lambda}_\mathrm{t} = [\lambda_{\mathrm{t}1}\ \lambda_{\mathrm{t}2}]^\mathrm{T}$ are the two components of the friction contact force. In this section, the model for contacts with friction is presented and the contact force is defined for one contact point.

Normal Force

The normal contact force is assumed to be non-negative,

$$\lambda_\mathrm{n} \geqslant 0 \tag{2}$$

and is usually defined as a kinematic constraint force, where the *gap function* ϕ is the constrained distance. This determines the distance between each contact pair, and so it has to be zero if the contact is established and positive when it detaches, therefore

$$\phi \geqslant 0 \tag{3}$$

In addition a *complementarity condition* between the contact force and the gap function is needed to make sure that no force is applied when the contact is detached, then

$$\lambda_\mathrm{n}\phi = 0 \tag{4}$$

This condition can also be applied to the normal velocity and acceleration of the contact point $\dot{\phi}$ and $\ddot{\phi}$, so that it can be introduced into the dynamic equations easily.

Friction Force

The Coulomb friction model is characterized by two phases: static and kinetic. In the static phase, friction acts as a constraint force with a maximum value, while in the kinetic phase, the force value only depends on the normal force and it opposes the sliding direction.

For the *static friction force*, let us define k different directions in the tangent plane, so that the *friction saturation* σ associated with the upper and lower bounds for each direction are

$$\sigma_{\mathrm{up}_j} = \mu_\mathrm{s}\lambda_\mathrm{n} - \mathbf{e}_j^\mathrm{T}\boldsymbol{\lambda}_\mathrm{t} \geqslant 0 \tag{5}$$

$$\sigma_{\mathrm{lo}_j} = \mu_\mathrm{s}\lambda_\mathrm{n} + \mathbf{e}_j^\mathrm{T}\boldsymbol{\lambda}_\mathrm{t} \geqslant 0 \tag{6}$$

where μ_s is the static friction coefficient, and $\mathbf{e}_j$ is the unit vector of the j-th direction.

If the static friction force is defined as a constraint force, the friction saturations must be complementary to the tangential acceleration component towards the opposite direction, so that the contact point can only transition to sliding if the friction force reaches the bounds. Let the tangent acceleration be

$$\dot{\mathbf{u}}_\mathrm{t} = \sum_{j=1}^{k} \left(\kappa_{\mathrm{up}_j}\mathbf{e}_j - \kappa_{\mathrm{lo}_j}\mathbf{e}_j \right) \tag{7}$$

where $\kappa_{\mathrm{up}_j} \geqslant 0$ and $\kappa_{\mathrm{lo}_j} \geqslant 0$ are the acceleration parameters pointing to the positive and negative directions of $\mathbf{e}_j$, respectively. The complementarity conditions are

$$\sigma_{\mathrm{up}_j}\kappa_{\mathrm{lo}_j} = 0 \tag{8}$$

$$\sigma_{\mathrm{lo}_j}\kappa_{\mathrm{up}_j} = 0 \tag{9}$$

However, the above definition of the friction saturation leads to an LCP with a rank-deficient lead matrix [4], because two bounds are defined for the same direction. Here, we propose a new definition for the friction saturations, which produces a full-rank LCP,

$$\tilde{\sigma}_{\mathrm{up}_j} = \mu_\mathrm{s}\lambda_\mathrm{n} - \mathbf{e}_j^\mathrm{T}\boldsymbol{\lambda}_\mathrm{t} + \rho\,\kappa_{\mathrm{up}_j} \geqslant 0 \tag{10}$$

$$\tilde{\sigma}_{\mathrm{lo}_j} = \mu_\mathrm{s}\lambda_\mathrm{n} + \mathbf{e}_j^\mathrm{T}\boldsymbol{\lambda}_\mathrm{t} + \rho\,\kappa_{\mathrm{lo}_j} \geqslant 0 \tag{11}$$

The novelty of this model is the addition of the *phantom inertia* ρ into the equations, which does not change the dynamics of the contact model, but it adds some extra information into

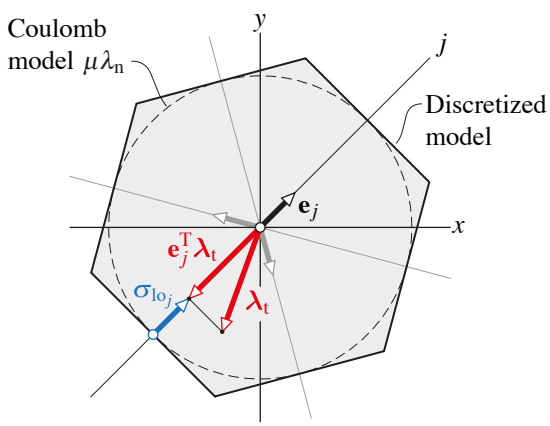

FIGURE 1. DISCRETIZED FRICTION MODEL (STICKING).

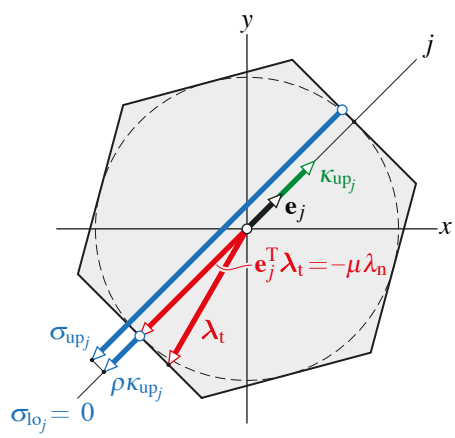

FIGURE 2. PHANTOM INERTIA IN STICK-SLIP TRANSITION.

the equations and makes the lead matrix of the LCP full rank. The complementarity conditions make sure that force and acceleration will never point to the same direction, even though this inertial term is used.

It can be shown that a solution where both parameters κ_{up_j} and κ_{lo_j} are positive is not possible, no matter how big ρ is. When the friction force reaches a bound, only the acceleration pointing to the opposite direction will be positive; and when the friction force is within the bounds of that direction, i.e., $|\mathbf{e}_j^T\boldsymbol{\lambda}_t| < \mu\lambda_n$, the two parameters $\kappa_{up_j} = \kappa_{lo_j} = 0$, see Figure 1. The inertia ρ only makes the friction saturation of one bound larger, in case the sliding starts in the opposite direction, and thus it does not influence the stick-slip transition, see Figure 2.

The *kinetic friction force* is defined as

$$\boldsymbol{\lambda}_t = -\mu_k\lambda_n\mathbf{e}_t \tag{12}$$

where μ_k is the kinetic friction coefficient, and $\mathbf{e}_t = \mathbf{u}_t/\|\mathbf{u}_t\|$ defines the sliding direction.

MULTIBODY FORMULATION

Let $\mathbf{q}$ be the $p\times 1$ array of generalized coordinates, and $\mathbf{v}$ a set of n generalized velocities of a multibody system, such that $\dot{\mathbf{q}} = \boldsymbol{\Gamma}\mathbf{v}$, where $\boldsymbol{\Gamma}(\mathbf{q},t)$ is the $p\times n$ transformation matrix. Then, the dynamic equations are

$$\mathbf{M}\dot{\mathbf{v}} + \mathbf{c} = \mathbf{f}_a + \mathbf{f}_b + \mathbf{f}_c \tag{13}$$

where $\mathbf{M}(\mathbf{q})$ is the $n\times n$ mass matrix, $\mathbf{c}(\mathbf{q},\mathbf{v})$ is the $n\times 1$ array containing the Coriolis and centrifugal terms, $\mathbf{f}_a$ are the generalized applied forces, $\mathbf{f}_b$ are the generalized bilateral constraint forces, and $\mathbf{f}_c$ are the generalized contact forces.

The bilateral holonomic constraints are arranged into the $m\times 1$ array $\boldsymbol{\Theta}(\mathbf{q}) = \mathbf{g}(t)$ and defined at the velocity level as

$$\mathbf{u}_b = \dot{\boldsymbol{\Theta}} = \mathbf{J}_b\mathbf{v} \tag{14}$$

where $\mathbf{J}_b(\mathbf{q}) = \frac{\partial\boldsymbol{\Theta}}{\partial\mathbf{q}}\boldsymbol{\Gamma}$ is the $m\times n$ constraint Jacobian matrix, and $\mathbf{u}(\mathbf{q},t)$ is a $m\times 1$ array of given functions, which are usually equal to zero. The generalized bilateral constraint force is then $\mathbf{f}_b = \mathbf{J}_b^T\boldsymbol{\lambda}_b$, where $\boldsymbol{\lambda}_b$ is the $m\times 1$ array of Lagrange multipliers, which represent the constraint forces and moments.

The *gap functions* of all the contact points are arranged into the $r\times 1$ array $\boldsymbol{\Phi}(\mathbf{q})$, and the normal separation velocity can be expressed as

$$\mathbf{u}_n = \dot{\boldsymbol{\Phi}} = \mathbf{J}_n\mathbf{v} \tag{15}$$

where $\mathbf{J}_n(\mathbf{q}) = \frac{\partial\boldsymbol{\Phi}}{\partial\mathbf{q}}\boldsymbol{\Gamma}$ is the $r\times n$ contact Jacobian matrix.

The tangent plane of each contact point is characterized using two orthogonal directions, in which the components of the sliding velocity at the contact points can be expressed as

$$\mathbf{u}_t = \mathbf{J}_t\mathbf{v} \tag{16}$$

where $\mathbf{J}_t(\mathbf{q})$ is the $2r\times n$ friction Jacobian matrix. Therefore, the generalized contact force is

$$\mathbf{f}_c = \mathbf{J}_n^T\boldsymbol{\lambda}_n + \mathbf{J}_t^T\boldsymbol{\lambda}_t \tag{17}$$

where $\boldsymbol{\lambda}_{\mathrm{n}}$ contains the r normal forces, and $\boldsymbol{\lambda}_{\mathrm{t}}$ contains the $2r$ components of the friction forces.

If a contact is sticking, the friction saturations in Eqns. (10) and (11) can be arranged in a matrix form, so that the 2 arrays of k_i friction saturations of the i-th contact point are

$$\tilde{\boldsymbol{\sigma}}_{\mathrm{up}_i} = \boldsymbol{\mu}_i \lambda_{\mathrm{n}_i} - \mathbf{E}_i^{\mathrm{T}} \boldsymbol{\lambda}_{\mathrm{t}_i} + \boldsymbol{\rho}_i \boldsymbol{\kappa}_{\mathrm{up}_i} \geqslant \mathbf{0} \tag{18}$$

$$\tilde{\boldsymbol{\sigma}}_{\mathrm{lo}_i} = \boldsymbol{\mu}_i \lambda_{\mathrm{n}_i} + \mathbf{E}_i^{\mathrm{T}} \boldsymbol{\lambda}_{\mathrm{t}_i} + \boldsymbol{\rho}_i \boldsymbol{\kappa}_{\mathrm{lo}_i} \geqslant \mathbf{0} \tag{19}$$

where $\boldsymbol{\mu}_{\mathrm{s}_i} = \left[\, \mu_{\mathrm{s}_i} \cdots \mu_{\mathrm{s}_i} \,\right]^{\mathrm{T}}$ are the friction coefficients, $\boldsymbol{\rho}_i = \mathrm{diag}\left(\rho_i, \ldots, \rho_i\right)$ are the phantom inertias, $\mathbf{E}_i = \left[\, \mathbf{e}_1 \cdots \mathbf{e}_{k_i} \,\right]$ are the components of the unit vectors of the directions used in the tangent plane for the discretized friction model, and $\boldsymbol{\kappa}_{\mathrm{up}_i}$ and $\boldsymbol{\kappa}_{\mathrm{lo}_i}$ contain the components used to parametrize the tangent acceleration

$$\dot{\mathbf{u}}_{\mathrm{t}_i} = \mathbf{E}_i \boldsymbol{\kappa}_{\mathrm{up}_i} - \mathbf{E}_i \boldsymbol{\kappa}_{\mathrm{lo}_i} \tag{20}$$

Otherwise, if a contact point is sliding, the kinetic friction force in Eqn. (12) gives a generalized contact force

$$\boldsymbol{\lambda}_{\mathrm{c}_i} = \left(\mathbf{J}_{\mathrm{n}_i}^{\mathrm{T}} - \mu_{\mathrm{k}_i} \mathbf{J}_{\mathrm{t}_i}^{\mathrm{T}} \mathbf{e}_{\mathrm{t}_i}\right) \lambda_{\mathrm{n}_i} = \mathbf{J}_{\mathrm{c}_i}^{\mathrm{T}} \lambda_{\mathrm{n}_i} \tag{21}$$

which allows the dynamic equations to formulate an LCP [4]. This expression of the generalized force $\mathbf{J}_{\mathrm{c}_i} \neq \mathbf{J}_{\mathrm{n}_i}$ is due to the Coulomb model, however, it may compromise the existance of solution of the LCP [4]. In some cases, the dynamic equations of rigid body systems under Coulomb friction can have no solution, or even multiple solutions; which gave rise to the *Painlevé paradox* [11].

Nevertheless, this friction model can be used in a time-stepping formulation at the velocity level, as it is shown below. This kind of formulations was proven to always have a solution [5, 6], because the Coulomb model is physically based. Although there is no solution for the forces and the acceleration of the system at a singular instant of time, there is a solution for the velocity at following instants and for the impulse developed by the contact force along time.

TIME-STEPPING

For the velocity-level formulation, a finite difference approximation is used to introduce the velocities into the equations, so that the unknown acceleration is

$$\dot{\mathbf{v}}^+ = \frac{\mathbf{v}^+ - \mathbf{v}}{h} \tag{22}$$

where $\mathbf{v}^+$ is the unknown velocity, and h is the time-step size. The superscript $^+$ denotes the unknown variables at each time-step, while the others are known or are computed using known values.

Similarly, the configuration of the system is updated at the end of the time-step as follows

$$\mathbf{q}^+ = \mathbf{q} + \boldsymbol{\Gamma}(\mathbf{q}) \mathbf{v}^+ \tag{23}$$

Multibody Formulation

Equation (13) can be written in terms of the unknown velocities as

$$\mathbf{M}\mathbf{v}^+ - \mathbf{J}_{\mathrm{b}} h \boldsymbol{\lambda}_{\mathrm{b}}^+ - \mathbf{J}_{\mathrm{t}} h \boldsymbol{\lambda}_{\mathrm{t}}^+ - \mathbf{J}_{\mathrm{n}} h \boldsymbol{\lambda}_{\mathrm{n}}^+ = \mathbf{b}_0 \tag{24}$$

where $\mathbf{b}_0 = \mathbf{M}\mathbf{v} - \mathbf{c} + \mathbf{f}_{\mathrm{a}}$, the mass matrix $\mathbf{M}$, and the Jacobian matrices $\mathbf{J}$, are computed using the known configuration $\mathbf{q}$ and velocity $\mathbf{v}$ at each time-step. Also, the bilateral constraints in Eqn. (14) become

$$\mathbf{u}_{\mathrm{b}}^+ = \mathbf{J}_{\mathrm{b}} \mathbf{v}^+ = \mathbf{0} \tag{25}$$

Contact Model

The unilateral constraints (i.e., contacts) are written at the velocity level as

$$\mathbf{u}_{\mathrm{n}}^+ = \mathbf{J}_{\mathrm{n}} \mathbf{v}^+ \geqslant \mathbf{0} \tag{26}$$

which are complementary to the contact forces $\boldsymbol{\lambda}_{\mathrm{n}}^+ \geqslant \mathbf{0}$ therefore,

$$u_{\mathrm{n}_i}^+ \lambda_{\mathrm{n}_i}^+ = 0 \quad \forall i = 1 \ldots r \tag{27}$$

A velocity threshold is used to determine if a contact point is sticking, and it is the case if $\|\mathbf{u}_{\mathrm{t}_i}\| < v_{\mathrm{s}}$, which means that $\mathbf{u}_{\mathrm{t}_i} \approx \mathbf{0}$. Additionally, from Eqn. (20), the unknown tangential velocity of the contact point can be expressed as

$$\mathbf{u}_{\mathrm{t}_i}^+ = \mathbf{J}_{\mathrm{t}_i} \mathbf{v}^+ = \mathbf{E}_i \mathbf{w}_{\mathrm{up}_i}^+ - \mathbf{E}_i \mathbf{w}_{\mathrm{lo}_i}^+ \tag{28}$$

where $\mathbf{w}_{\mathrm{up}_i}^+ = h \boldsymbol{\kappa}_{\mathrm{up}_i} \geqslant \mathbf{0}$ and $\mathbf{w}_{\mathrm{lo}_i}^+ = h \boldsymbol{\kappa}_{\mathrm{lo}_i} \geqslant \mathbf{0}$ parametrize the tangential velocity in each direction. Then, the friction saturations in Eqns. (18) and (19) are written in terms of the impulses and the unknown sliding velocity

$$h \tilde{\boldsymbol{\sigma}}_{\mathrm{up}_i}^+ = \boldsymbol{\mu}_i h \boldsymbol{\lambda}_{\mathrm{n}_i}^+ - \mathbf{E}_i^{\mathrm{T}} h \boldsymbol{\lambda}_{\mathrm{t}_i}^+ + \boldsymbol{\rho}_i \mathbf{w}_{\mathrm{up}_i}^+ \geqslant \mathbf{0} \tag{29}$$

$$h \tilde{\boldsymbol{\sigma}}_{\mathrm{lo}_i}^+ = \boldsymbol{\mu}_i h \boldsymbol{\lambda}_{\mathrm{n}_i}^+ + \mathbf{E}_i^{\mathrm{T}} h \boldsymbol{\lambda}_{\mathrm{t}_i}^+ + \boldsymbol{\rho}_i \mathbf{w}_{\mathrm{lo}_i}^+ \geqslant \mathbf{0} \tag{30}$$

which, according to Eqns. (8) and (9), are complementary to the velocity parameters $\mathbf{w}^{+}_{\mathrm{lo}_i} \geqslant \mathbf{0}$ and $\mathbf{w}^{+}_{\mathrm{up}_i} \geqslant \mathbf{0}$, respectively.

If the contact point is sliding (i.e., $\|\mathbf{u}_{\mathrm{t}_i}\| \geqslant v_{\mathrm{s}}$), one option is to parametrize the sliding velocity using the sliding and lateral directions

$$\mathbf{u}^{+}_{\mathrm{t}_i} = \left[\, \mathbf{e}_{\mathrm{t}_i}\, \mathbf{e}_{\mathrm{l}_i} \,\right] \mathbf{w}^{+}_{\mathrm{up}_i} - \left[\, \mathbf{e}_{\mathrm{t}_i}\, \mathbf{e}_{\mathrm{l}_i} \,\right] \mathbf{w}^{+}_{\mathrm{lo}_i} \tag{31}$$

where $\mathbf{e}_{\mathrm{t}_i}$ and $\mathbf{e}_{\mathrm{l}_i}$ are the unit vectors of the sliding and lateral directions, respectively, and $\mathbf{w}^{+}_{\mathrm{up}_i}$ and $\mathbf{w}^{+}_{\mathrm{lo}_i}$ are the parameters of the sliding velocity. Then, the friction force can be defined component-wise as

$$\mathbf{e}^{\mathrm{T}}_{\mathrm{t}_i} \boldsymbol{\lambda}^{+}_{\mathrm{t}_i} = -\mu_{\mathrm{k}_i} \lambda^{+}_{\mathrm{n}_i} \tag{32}$$

$$\mathbf{e}^{\mathrm{T}}_{\mathrm{l}_i} \boldsymbol{\lambda}^{+}_{\mathrm{t}_i} = 0 \tag{33}$$

so that the force follows the Coulomb law of Eqn. (12).

However, there are two main problems that can arise when using the above definition for the kinetic friction force. On the one hand, applying the friction force based on the known sliding velocity $\mathbf{u}_{\mathrm{t}_i}$ may compromise a slip-stick transition and produce an oscillation of the contact point about zero velocity. Therefore, if the applied kinetic force is so large that it would make the sliding velocity change to the opposite direction, a slip-stick transition has to happen and the friction force needs to make the sliding velocity equal to zero. This can be accomplished by defining two friction saturations similarly to the ones in Eqns. (30) and (29) for the sliding and lateral directions, but using

$$\mathbf{E}_i = \left[\, \mathbf{e}_{\mathrm{t}_i}\, \mathbf{e}_{\mathrm{l}_i} \,\right] \quad \text{and} \quad \boldsymbol{\mu}_i = \begin{bmatrix} \mu_{k_i} \\ 0 \end{bmatrix} \tag{34}$$

so that they become Eqns. (32) and (33) if the component along the sliding direction $w_{\mathrm{up}_i} > 0$.

On the other hand, not applying a force in the lateral direction allows the sliding velocity to change in that direction, and so the misalignment between force and velocity may become significant and even induce some vibrations in the system. That is why, some authors have used the same approach as for the static friction and define k_i directions in the tangent plane, and friction saturation for each. However, this increases the size of the system unnecessarily if the sliding velocity is very large, because the the friction force would not change much the direction. In the next section, an alternative approach to reduce the misalignment will be shown by using a force regularization without increasing the system size.

LINEAR COMPLEMENTARITY PROBLEM (LCP)

To formulate an LCP, Equation (24) together with the constraint Eqns. (25) and (26), the tangent velocity Eqn. (28) and the friction saturation Eqns. (29) and (30), are arranged in the following matrix for

$$\begin{bmatrix} \mathbf{M} & -\mathbf{J}^{\mathrm{T}}_{\mathrm{b}} & -\mathbf{J}^{\mathrm{T}}_{\mathrm{t}} & -\mathbf{J}^{\mathrm{T}}_{\mathrm{n}} & \mathbf{0} & \mathbf{0} \\ \mathbf{J}_{\mathrm{b}} & \mathbf{0} & \mathbf{0} & \mathbf{0} & \mathbf{0} & \mathbf{0} \\ \mathbf{J}_{\mathrm{t}} & \mathbf{0} & \mathbf{0} & \mathbf{0} & -\mathbf{E} & \mathbf{E} \\ \mathbf{J}_{\mathrm{n}} & \mathbf{0} & \mathbf{0} & \mathbf{0} & \mathbf{0} & \mathbf{0} \\ \mathbf{0} & \mathbf{0} & \mathbf{E}^{\mathrm{T}} & \boldsymbol{\mu} & \mathbf{0} & \boldsymbol{\rho} \\ \mathbf{0} & \mathbf{0} & -\mathbf{E}^{\mathrm{T}} & \boldsymbol{\mu} & \boldsymbol{\rho} & \mathbf{0} \end{bmatrix} \begin{bmatrix} \mathbf{v} \\ h\boldsymbol{\lambda}_{\mathrm{b}} \\ h\boldsymbol{\lambda}_{\mathrm{t}} \\ h\boldsymbol{\lambda}_{\mathrm{n}} \\ \mathbf{w}_{\mathrm{up}} \\ \mathbf{w}_{\mathrm{lo}} \end{bmatrix}^{+} + \mathbf{d} = \begin{bmatrix} \mathbf{0} \\ \mathbf{0} \\ \mathbf{0} \\ \mathbf{u}_{\mathrm{n}} \\ h\tilde{\boldsymbol{\sigma}}_{\mathrm{lo}} \\ h\tilde{\boldsymbol{\sigma}}_{\mathrm{up}} \end{bmatrix}^{+} \tag{35}$$

where $\mathbf{E} = \mathrm{diag}\left(\mathbf{E}_1, \ldots, \mathbf{E}_r\right)$, $\boldsymbol{\mu} = \mathrm{diag}\left(\boldsymbol{\mu}_1, \ldots, \boldsymbol{\mu}_r\right)$, $\boldsymbol{\rho} = \mathrm{diag}\left(\boldsymbol{\rho}_1, \ldots, \boldsymbol{\rho}_r\right)$, and the complementary variables are

$$\boldsymbol{\lambda}_{\mathrm{n}} \geqslant \mathbf{0} \quad \text{compl. to} \quad \mathbf{u}_{\mathrm{n}} \geqslant \mathbf{0} \tag{36}$$

$$\mathbf{w}_{\mathrm{up}} \geqslant \mathbf{0} \quad \text{compl. to} \quad \tilde{\boldsymbol{\sigma}}_{\mathrm{lo}} \geqslant \mathbf{0} \tag{37}$$

$$\mathbf{w}_{\mathrm{lo}} \geqslant \mathbf{0} \quad \text{compl. to} \quad \tilde{\boldsymbol{\sigma}}_{\mathrm{up}} \geqslant \mathbf{0} \tag{38}$$

which formulate an LCP via eliminating the variables $\dot{\mathbf{v}}$, $\boldsymbol{\lambda}_{\mathrm{b}}$ and $\boldsymbol{\lambda}_{\mathrm{t}}$, using the Schur complement.

The role of the square diagonal *phantom inertia* matrix $\boldsymbol{\rho}$ is clearly shown in Eqn. (35). Due to the use of dependent directions to discretize the friction cone, the two last block columns of the lead matrix would be linearly dependent. However, the discrete friction model proposed here gives rise to a full-rank LCP formulation, by coupling the friction saturations without changing the dynamics of the system. If the contact forces are not redundant, the normal and friction contact Jacobian matrices are full-rank, and so is the lead matrix. Nevertheless, if the system presents redundancy, some physics-based techniques (e.g., constraint relaxation) would be required to solve the dynamic equations and determine the contact forces.

Constraint Relaxation

In case that the system presents redundancy, the constraints can be relaxed, so that the dynamic equations can be solved. This is done by introducing the so called *relaxation terms* in some diagonal elements of the LCP lead matrix, which becomes

$$\begin{bmatrix} \mathbf{M} & -\mathbf{J}^{\mathrm{T}} & \mathbf{0} \\ \mathbf{J} & \boldsymbol{\varepsilon} & \mathbf{H} \\ \mathbf{0} & -\mathbf{H}^{\mathrm{T}} & \mathbf{N} \end{bmatrix} \begin{bmatrix} \mathbf{v} \\ h\boldsymbol{\lambda} \\ \tilde{\mathbf{w}} \end{bmatrix}^{+} + \mathbf{d} = \begin{bmatrix} \mathbf{0} \\ \tilde{\mathbf{u}} \\ h\tilde{\boldsymbol{\sigma}} \end{bmatrix}^{+} \tag{39}$$

where $\boldsymbol{\varepsilon}$ is a diagonal matrix containing the relaxation terms. When relaxing the constraints, the elements in the vector $\mathbf{d}$ change, and so does the meaning of the velocities $\tilde{\mathbf{w}}$ and $\tilde{\mathbf{u}}$.

For each constraint force (i.e., bilateral constraint, and normal and friction constraint forces), a relaxation term can be defined as [7, 12]

$$\varepsilon_i = \left(k_i h^2 + b_i h\right)^{-1} \tag{40}$$

where k_i and b_i are the stiffness and damping associated with the constraint, respectively. In addition, the terms

$$d_i = \varepsilon_i h k_i \delta_i - u_i \tag{41}$$

where δ_i and u_i account for the position and velocity violation of the constraint. For the bilateral constraints, $\delta_i = \theta_i - g_i$ and $u_i = \dot{g}_i$, from Eqn. (14). For the normal contact force, $\delta_i = \phi_i$, the gap function, and $u_i = 0$.

On the other hand, the friction force can also be regularized using a linear stiffness and damping by following a bristle model approach [12, 13]. In such a case, the relaxation term has the same expression as the one above, and the terms in $\mathbf{d}$ for both directions in the tangent plane are

$$\mathbf{d}_i = -\varepsilon_i h \left(\boldsymbol{\lambda}_{\mathrm{t}_i} + b_i \mathbf{u}_{\mathrm{t}_i}\right) \tag{42}$$

where $\boldsymbol{\lambda}_{\mathrm{t}_i}$ and $\mathbf{u}_{\mathrm{t}_i}$ are the friction force and tangential velocity from the previous time-step, respectively.

Moreover, as mentioned before, the misalignment between the sliding velocity and the kinetic friction force can be reduced via a force regularitzation in the lateral direction [12]. To do so, the directions defining the sliding velocity need to be aligned with the sliding and lateral direction, so that the elements defined in Eqn. (34) are $\mathbf{E}_i = \mathbf{I}$, the 2×2 identity matrix, and $\boldsymbol{\mu}_i = [\mu_{\mathrm{k}_i}\ \mu_{\mathrm{k}_i}]^{\mathrm{T}}$. Then, the relaxation term for the lateral direction is

$$\varepsilon_{\mathrm{l}_i} = \frac{u_{\mathrm{t}_i}}{\mu_{\mathrm{k}_i} \lambda_{\mathrm{t}_i} h} \tag{43}$$

where λ_{n_i} and $u_{\mathrm{t}_i} = \|\mathbf{u}_{\mathrm{t}_i}\|$ are the normal force and sliding velocity from the previous time-step.

EXAMPLE

In order to compare the velocity-level formulation with other existing formulations, a cube-shaped rigid body has been simulated. Initial conditions have been given to the system so that it slides on a fixed flat ground for a while until it stops, see Figure 3. To model the contact, four contact points at the vertices have been considered. Table 1 shows the system properties.

The formulations used to compare the results are the Anitescu and Potra (AP) [6], the Box friction model [7], and the Hybrid regularized friction model [12]. Figure 4 shows the trajectory of the centre of mass of the body, and as it can be seen all of them show the same behaviour. In [12], it was shown that the Hybrid model had significantly less error than the other existing formulations, compared to the Coulomb friction model. For the example presented here, the trajectory of the proposed model is the closest to the Hybrid model, and thus, closer to the Coulomb model than the others.

TABLE 1. BOX ON THE GROUND EXAMPLE PROPERTIES.

Body		
Mass	m	1 kg
Side Length	l	1 m
Initial conditions		
Velocity of the CoG	v_y	5 m/s
Angular Velocity	ω_z	2π s^{-1}
Contact Parameters		
Stiffness	k_{n}	10^{10} N/m
Damping	b_{n}	10^{8} Ns/m
Friction Parameters		
Friction Coefficient	μ	1
Stiffness	k_{t}	10^{8} N/m
Damping	b_{t}	10^{5} Ns/m
Velocity Threshold	v_{th}	0.001 m/s

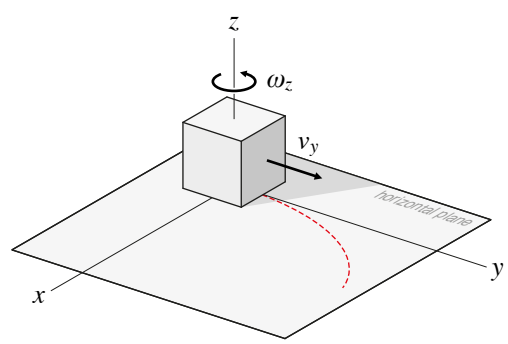

FIGURE 3. BOX ON THE GROUND EXAMPLE.

The method used to solve the LCP depends on each formulation. AP formulation can only be solved using Lemke's algorithm [6] because the lead matrix is rank-deficient. On the other hand, others have been solved with the algorithm proposed by Júdice and Pires [10], because it can deal with mixed LCPs. This method can only deal with full-rank LCPs, and it has been used with the new formulation to show that it is full-rank thanks to the friction model proposed here.

It is worth mentioning that, in all the formulations, the tan-

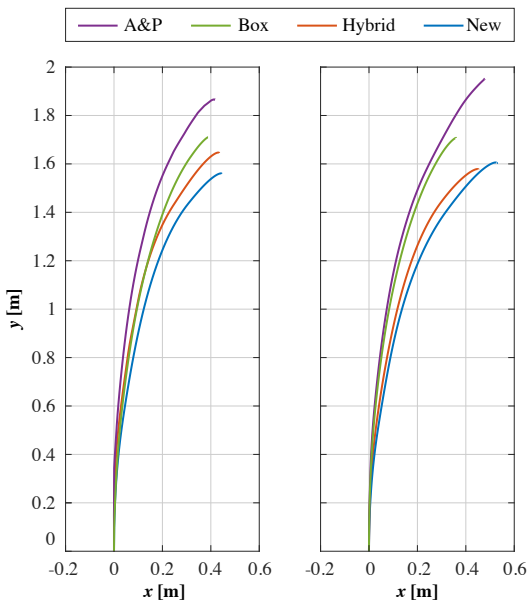

FIGURE 4. BOX ON THE GROUND EXAMPLE RESULTS. TIME-STEP SIZE: 10 ms (LEFT), 1 ms (RIGHT).

gent plane is discretized by two orthogonal directions, which is the only option for the Box and Hybrid formulations. Nevertheless, many directions can be used to define the tangent plane in the other formulations, which would result in a better approximation of the Coulomb model. It has been noticed that the formulation proposed here shows some problems when using block-pivoting algorithms (e.g., [10]) if more than two directions in the tangent plane are used. The pivoting step might try to solve a rank-deficient system if many variables are pivoted at the same time. However, there are no issues when solving it with single-pivoting algorithms, such as Lemke's.

As expected, the *phantom inertia* introduced in the friction model has not shown any significant effect on either the dynamics or the performance of the simulations. However, it is highly recommended not to use very small values, so that the matrix does not become ill-conditioned. For the system at hand, the LCP becomes rank-deficient for values of $\rho < 10^{-8}$ kg.

CONCLUSIONS

The velocity-level formulation proposed here has a similar performance compared to the other existing LCP-based formulations, but it approximates the Coulomb model better than the other existing formulations. Moreover, the bounds of the static friction force are coupled with the normal force, which is not the case in other formulations.

In addition, since it has a non-singular lead matrix, any algorithm available in the literature is able to solve it. However, especial attention needs to be paid when defining many directions in the tangent plane to discretize the friction model if block-pivoting algorithms are used.

As the main novelty of the model, the inertial terms added to the friction model have shown to be very effective in augmenting the rank of the LPC lead matrix, while keeping a similar behaviour of the model compared to other discretized friction models.

REFERENCES

[1] Moreau, J., 1966. "Quadratic programming in mechanics: Dynamics of one sided constraints". *SIAM Journal on Control,* ***4***(1), pp. 153–158.

[2] Lötstedt, P., 1982. "Mechanical systems of rigid bodies subject to unilateral constraints". *SIAM Journal of Applied Mathematics,* ***42***(2), pp. 281–296.

[3] Anitescu, M., and Tasora, A., 2010. "An iterative approach for cone complementarity problems for nonsmooth dynamics". *Computational Optimization and Applications,* ***47***, pp. 207–235.

[4] Glocker, C., 2001. *Set-Valued Force Laws*. Springer, Troy, New York, USA.

[5] Stewart, D. E., and Trinkle, J. C., 1996. "An implicit time-stepping scheme for rigid body dynamics with inelastic collisions and coulomb friction". *International Journal for Numerical Methods in Engineering,* ***39***, pp. 2673–2691.

[6] Anitescu, M., and Potra, F. A., 1997. "Formulating dynamic multi-rigid-body contact problems with friction as solvable linear complementarity problems". *Nonlinear Dynamics,* ***14***, pp. 231–247.

[7] Lacoursière, C., 2006. A regularized time stepper for multibody systems. Tech. Rep. 04, UMINF.

[8] Cottle, R. W., and Dantzig, G., 1968. "Complementarity pivot theory of mathematical programming". *Linear Algebra and its Applications,* ***1***, pp. 103–125.

[9] Murty, K., 1988. *Linear Complementarity, Linear and Nonlinear Programming*. Heldermann, Berlin, Germany.

[10] Júdice, J., and Pires, F., 1992. "Basic-set algorithm for a generalized linear complementarity problem". *Journal of optimization theory and applications,* ***74***(3), pp. 391–411.

[11] Génot, F., and Brogliato, B., 1998. New Results on Painlevé Paradoxes. Tech. Rep. RR-3366, INRIA.

[12] Peiret, A., Gholami, F., Kövecses, J., and Font-Llagunes, J. M., 2016. "A regularized contact model for multibody system simulation". In ASME 2016 International Design Engineering Technical Conferences & Computers and Information in Engineering Conference.

[13] Liang, J., Fillmore, S., and Ma, O., 2012. "An extended bristle friction force model with experimental validation". *Mechanism and Machine Theory,* ***56***, pp. 123–137.